

Iminoxyl radicals and stable products from the one-electron oxidation of 1-methylindole-3-carbaldehyde oximes

2 PERKIN

Steven A. Everett,^{*a} Matthew A. Naylor,^a Michael R. L. Stratford,^a Kantilal B. Patel,^a Eleonora Ford,^a Alan Mortensen,^b Amanda C. Ferguson,^a Borivoj Vojnovic^a and Peter Wardman^a

^a Gray Cancer Institute, PO Box 100, Mount Vernon Hospital, Northwood, Middlesex, UK HA6 2JR. E-mail: everett@graylab.ac.uk

^b Royal Veterinary and Agricultural University, Rolighedsvej 30, DK-1958 Frederiksberg C, Denmark

Received (in Cambridge, UK) 28th March 2001, Accepted 1st August 2001

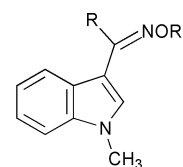
First published as an Advance Article on the web 12th September 2001

The radical intermediates and the stable products formed on one-electron oxidation of 1-methylindole-3-carbaldehyde oxime **2a** were compared with those of 1-methylindole-3-carboxamide oxime **4a** in aqueous solution. The dibromide radical anion generated radiolytically by pulse radiolysis reacted with both **2a** and **4a** $>C=NOH$ to yield the radical cations $[>C=NOH]^{\bullet+}$, which exist in prototropic equilibria with the neutral iminoxyl radicals $[>C=NO]^{\bullet}$ ($pK_a = 3.53 \pm 0.03$ and 5.01 ± 0.01 at ionic strength 0.05 M, respectively). This was confirmed by the observed primary salt-effect which accelerated the decay of the radical cations but not the iminoxyl radicals. Methylation of the *N*-hydroxyimino function in both **2a** and **4a** precluded deprotonation of the corresponding radical cations $[>C=NOCH_3]^{\bullet+}$. At low concentrations of **2a** and high dose rates the **2a** radicals $[>C=NO]^{\bullet}$ decayed bimolecularly *via* unstable dimers to the aldehyde $>C=O$, with higher concentrations and lower dose rates favouring the chain-catalysed isomerisation of the *N*-hydroxyimino moiety. Radicals from **4a** decay bimolecularly to form unstable dimers which degrade to produce an amide, nitrile and carboxylic acid. The observed differences in the oxidation chemistry of **2a** and **4a** probably reflect the enhanced stabilisation of iminoxyl radicals through α -amino substitution.

Introduction

Iminoxyl radicals ($>C=NO^{\bullet}$) were first characterised by Thomas in 1964 using electron paramagnetic resonance (EPR) spectroscopy.¹ Since then a number of EPR studies have been reported utilising a range of chemical^{1–6} and enzymatic systems^{7,8} for the oxidation of alkyl/aryl oximes to iminoxyl radicals. Other approaches rely on radical-addition to aromatic nitrile oxides.⁹ The iminoxyl radical is also formed when nitric oxide interacts with the tyrosine radical of photosystem II¹⁰ and the tyrosyl radical of prostaglandin H synthase-2.¹¹ In all cases, EPR spectroscopy has been valuable in detecting iminoxyl radicals which are characterised by a large splitting, $a_N \approx 30$ G, due to nitrogen. The electronic structure of iminoxyl radicals, as deduced from EPR spectra, place the unpaired electron in a π -type orbital derived from a nitrogen sp^2 orbital and an oxygen p orbital. This π -type orbital is believed to lie in the nodal plane of the $C=N$ π bond, which requires it to be orthogonal to the molecular π system, so that iminoxyl radicals have been described as σ radicals. Iminoxyl-type radicals (both *O*- and *N*-centred radicals) are possible candidates in the nitric oxide synthase (NOS)-catalysed oxidation of *N*^G-hydroxy-L-arginine to nitric oxide and citrulline.^{12,13} They are also believed to be putative intermediates in the oxidation of aryl oximes by cytochrome P450 mono-oxygenases^{14,15} and NOS.¹⁶

In the present work the technique of pulse radiolysis has been utilised, in which a known concentration of free radicals is generated in less than a microsecond, to study the one-electron oxidation of 1-methylindole-3-carbaldehyde oxime derivatives (see Fig. 1) by the dibromide radical anion ($Br_2^{\bullet-}$). Pulse radiolysis has been used extensively to study the spectral characteristics, acid–base, and redox properties of radicals from



Compound	R	R'
2a	H	H
4a	NH ₂	H
5	NH ₂	CH ₃
6	H	CH ₃

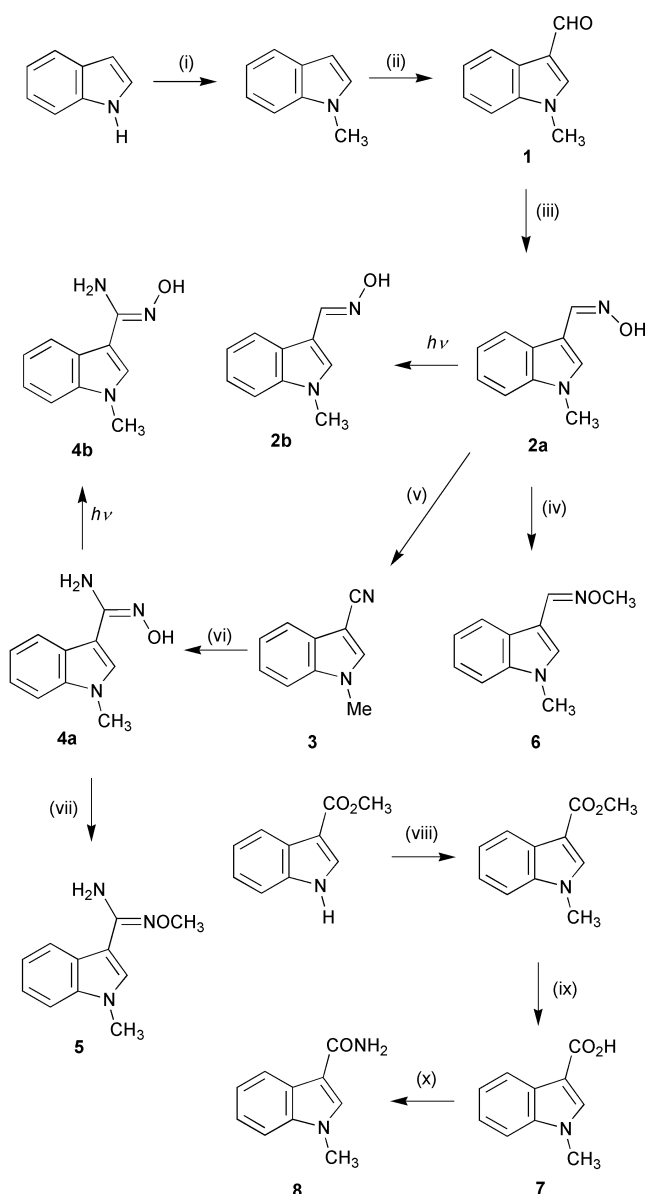
Fig. 1 Structures of 1-methylindole-3-carbaldehyde oxime derivatives.

the oxidation of indole-based compounds. For example, the radical cations of tryptophan¹⁷ and indole-3-acetic acids can deprotonate to form indolyl radicals, the latter case in competition with oxidative decarboxylation to form the skatole radical.^{18–22} The radical cation of *N*-methylindole is not believed to deprotonate over the pH range of interest in this study^{22–24} so the indole oximes (Fig. 1) have been *N*¹-methylated in order to study their iminoxyl radicals in isolation. Steady-state γ -radiolysis has been used to generate free radicals at a known, constant rate and, in combination with liquid chromatography, to study the stable products of free radical reactions and determine their yields relative to the precursor free radicals. α -Amino substitution in 1-methylindole-3-carbaldehyde oxime **2a** (to generate 1-methylindole-3-carboxamide oxime **4a**) has a significant impact on both the physico-chemical properties of the iminoxyl radicals and the subsequent product profiles.

Results and discussion

Synthetic chemistry

The synthetic pathways to 1-methylindole-3-carbaldehyde oxime derivatives and their oxidation products are outlined in Scheme 1. Methylation and Vilsmier formylation were followed by reaction with hydroxylamine to furnish the required aldehyde oxime **2a**. The *N*-hydroxyimino group exhibits (*Z*)-geometry relative to the indole core as determined by X-ray crystallography.²⁵ Photolysis of **2a** resulted in a stoichiometric conversion to the corresponding geometric (*E*)-isomer **2b**.²⁶ The sodium salt of **2a** was *O*-methylated with iodomethane to give **6**. Aldehyde oxime **2a** was dehydrated to give the nitrile **3** with refluxing acetic anhydride–sodium acetate and this material was treated with hydroxylamine to give the required carboxamide oxime **4a** which was then converted into **4b** by photolysis. This oxime could not be *O*-methylated with iodomethane *via* its sodium salt but the *O*-methyl derivative **5** was synthesised in low yield using trimethylxonium tetrafluoroborate. The putative oxidation product, amide **8**, was prepared from methyl indole-3-carboxylate by methylation and



Scheme 1 Synthesis of 1-methylindole-3-carbaldehyde oxime derivatives. Reagents and conditions: (i) NaH–MeI; (ii) POCl₃–DMF; (iii) NH₂OH–EtOH; (iv) NaH–MeI; (v) Ac₂O–NaOAc; (vi) NH₂OH–MeOH; (vii) (Me)₃OBf₄; (viii) NaH–MeI; (ix) KOH–MeCN–H₂O; (x) CDI–DMF, NH₃.

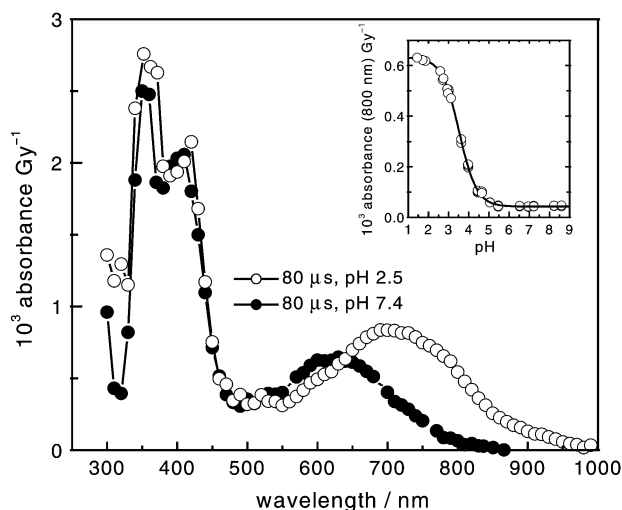


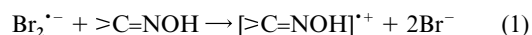
Fig. 2 Absorption spectrum of the radical cation (●) and the iminoxyl radical (○) measured by pulse radiolysis (30 μs after *ca.* 10 Gy pulses, 2 cm cell) of N₂O-saturated solutions of the oxime **2a** (100 μmol dm⁻³) and KBr (50 mmol dm⁻³) in phosphate buffer (4 mmol dm⁻³) at pH 3.5 and 7.4, respectively. The insert shows the change in absorbance at 800 nm of the radical cation as a function of pH fitted to the appropriate function. The data have been corrected for the decline in the dibromide radical yield at pH < 3.

hydrolysis to the free acid followed by treatment with carbonyl-diimidazole and then ammonia.

Free radical chemistry

The transient species formed by the one-electron oxidation of the oximes **2a**, **4a** and their corresponding *O*-methylated derivatives **6** and **5** by the dibromide radical anion (Br₂^{•-}, *E*^o = 1.66 V vs. NHE) were studied by pulse radiolysis. Spectral characteristics, prototropic equilibria and rate constants for the formation and decay of radicals are displayed in Table 1.

One-electron oxidation of 1-methylindole-3-carbaldehyde oxime 2a. The dibromide radical has a strong absorption in the wavelength range *ca.* 300–500 nm (*λ*_{max} = 360 nm).²⁷ In the absence of **2a**, the Br₂^{•-} radical decayed by a second-order process with a first half-life of *ca.* 0.2 ms, at an initial concentration of *ca.* 2.5 μmol dm⁻³. In the presence of 25–100 μmol dm⁻³ **2a** and at pH 7.4, the decay of the Br₂^{•-} radical, monitored by the decrease in absorption at 360 nm, followed pseudo-first-order kinetics with a rate constant proportional to the concentration of **2a**. An increase in absorption at 630 nm with the same rate constant (±10) was observed. These results indicated that the Br₂^{•-} radical reacts with **2a**; the rate constant for the reaction (1), obtained from the slope of the linear plot of pseudo-first-



order rate constant of the build-up of absorption at 630 nm *versus* concentration of **2a**, was *k*₁ = (8.2 ± 0.2) × 10⁸ dm³ mol⁻¹ s⁻¹ at ionic strength *ca.* 0.05 mol dm⁻³.

The absorption spectra of the radicals from the oxidation of **2a** were determined at pH 2.5 and 7.4 and are shown in Fig. 2. At pH 2.5 two maxima are observed at 350 and 705 nm, with extinction coefficients 2868 and 604 dm³ mol⁻¹ cm⁻¹, respectively. This spectrum is attributed to the radical cation **2a** [*>*C=NOH]^{•+} formed *via* reaction (1). In neutral solution the radical cation deprotonates to the neutral iminoxyl radical **2a** [*>*C=NO][•] the spectrum of which is characterised by two absorption maxima at 350 and 620 nm, with extinction coefficients of 1810 and 420 dm³ mol⁻¹ cm⁻¹, respectively.

Confirmation that the absorption spectra in Fig. 2 were

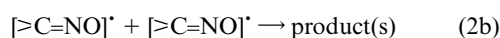
Table 1 Spectroscopic characteristics, prototropic equilibria and rate constants^a for the formation and decay of radicals generated by the oxidation of 1-methyl-3-carbaldehyde oxime derivatives by the Br₂^{•-} radical anion

Radical species	pH	λ_{\max}/nm	$\epsilon_{\max}/\text{M}^{-1}\text{cm}^{-1}$	Radical pK _a	$k_1/10^8\text{ dm}^3\text{ mol}^{-1}\text{ s}^{-1}$		$2k_{2a/2b}/10^6\text{ dm}^3\text{ mol}^{-1}\text{ s}^{-1}$	
					H ₂ O	D ₂ O	-NaClO ₄	+NaClO ₄ ^b
2a ^{•+}	2.5	350	2868 ± 50	3.53 ± 0.03	8.2	7.9	0.57	1.56
		705	604 ± 20					
2a(-H) [•]	5–9.5	350	1800 ± 50	5.7	5.5	1.24	1.12	
		620	420 ± 20					
4a ^{•+}	3	335	2180 ± 100	6.5	6.4	1.1	2.53	
		670	350 ± 20					
4a(-H) [•]	7–9.5	330	1700 ± 40	5.01 ± 0.05	4.6	4.6	1.0	1.1
		580	330 ± 170					
6 ^{•+}	3–9	340	2575 ± 200	None	4.1	3.8	2.1	5.5
		720	520 ± 180					
5 ^{•+}	3–9	350	2200 ± 200	None	2.3	2.1	1.6	2.8
		750	410 ± 20					

^a Rate constants in H₂O are subject to a standard deviation of 10% and in D₂O of 15%. ^b [NaClO₄] ≈ 500 mmol dm⁻³.

indeed due to the formation of the radical cation **2a** [$\text{>C=NOH}^{\bullet+}$] and the iminoxyl radical **2a** [>C=NO^{\bullet}] was achieved by studying the kinetic isotope-effect in heavy water (D₂O) on the formation kinetics and the primary salt-effect on the decay kinetics of these radicals. At pH 2.5, the rate constant for the oxidation of **2a** in D₂O was similar to that in H₂O within experimental error, $k_1 = (8.2 \pm 0.2) \times 10^8\text{ dm}^3\text{ mol}^{-1}\text{ s}^{-1}$ and $(7.9 \pm 0.2) \times 10^8\text{ dm}^3\text{ mol}^{-1}\text{ s}^{-1}$, respectively. The ratio of rate constants k_1 for the oxidation of **2a** by the Br₂^{•-} radical in H₂O and D₂O is 0.963, a value which is significantly higher than the ratio of viscosities of H₂O and D₂O, which is 0.8904 cP/1.0952 cP or 0.813.^{24,28} The absence of a measurable kinetic isotope effect argues against a hydrogen atom transfer mechanism in favour of an electron-transfer mechanism to generate the radical cation **2a** [$\text{>C=NOH}^{\bullet+}$] as illustrated by reaction (1).

At both pH 2.7 and 7.4 and low concentrations of **2a** ($[\mathbf{2a}] \approx 50\text{ }\mu\text{mol dm}^{-3}$), the radicals decayed on a millisecond timescale with second-order kinetics, where the rate of decay increased proportionately with the radical concentration (1–15 $\mu\text{mol dm}^{-3}$). At pH 2.7, the rate constant $2k_{2a} = (5.7 \pm 0.2) \times 10^5\text{ dm}^3\text{ mol}^{-1}\text{ s}^{-1}$ for bimolecular decay of the radical cation **2a** [$\text{>C=NOH}^{\bullet+}$] via reaction (2a) was obtained from the slope of the linear plot of the inverse of the first half-life ($= 2k_{2a} \times \text{initial concentration}$) for the decay in absorbance at 720 nm versus the initial radical concentration.



The inclusion of 0.5 mol dm⁻³ NaClO₄ increased the rate of radical decay by a factor of 2.7 to $2k_{2a} = (1.6 \pm 0.2) \times 10^6\text{ dm}^3\text{ mol}^{-1}\text{ s}^{-1}$ and is broadly consistent with the acceleration of the rate of decay of a species with net charge ±1, namely the radical cation **2a** [$\text{>C=NOH}^{\bullet+}$]. [According to the Debye–Hückel–Brønsted–Davis equation²⁹ the rate of second-order decay of a charged radical (either monocationic or mononegative) would have increased by a factor of 1.8, a value lower than determined experimentally, but the formula is not expected to be accurate at such a high ionic strength]. As expected, the increased salt concentration had a negligible effect on the decay of the neutral iminoxyl radical **2a** [>C=NO^{\bullet}] via reaction (2b): the values obtained in the absence and presence of 0.5 mol dm⁻³ NaClO₄ were determined to be $2k_{2b} = (1.2 \pm 0.4) \times 10^6$ and $(1.1 \pm 0.2) \times 10^6\text{ dm}^3\text{ mol}^{-1}\text{ s}^{-1}$, respectively.

The decay kinetics of the radical cation **2a** [$\text{>C=NOH}^{\bullet+}$] was independent of the concentration of **2a** from 0.05 to 1 mmol dm⁻³. However, at pH 7.4 the decay of the iminoxyl radicals **2a** [>C=NO^{\bullet}] was slower and began to deviate from both first-order

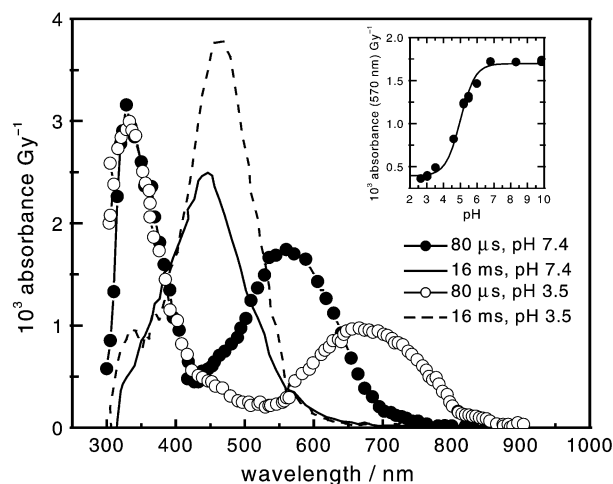
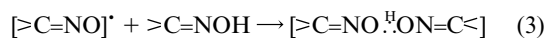


Fig. 3 Absorption spectrum of the radical cation (○) and the iminoxyl radical (●) measured by pulse radiolysis (80 μs after ca. 10 Gy pulses, 2 cm cell) of N₂O-saturated solutions of the amidoxime **4a** (100 $\mu\text{mol dm}^{-3}$) and KBr (50 mmol dm⁻³) in phosphate buffer (4 mmol dm⁻³) at pH 3.5 and 7.4, respectively. The dashed and solid lines represent products formed on dimerisation of the radical cation and iminoxyl radicals at pH 3.5 and pH 7.4, respectively. The insert shows the change in absorbance at 570 nm of the iminoxyl radical as a function of pH fitted to the appropriate function.

and second-order kinetics, particularly at low initial radical concentrations and higher **2a** concentration ($[\mathbf{2a}] \approx 1\text{ mmol dm}^{-3}$). The product analysis discussed later provides evidence that iminoxyl radical **2a** [>C=NO^{\bullet}] can initiate and propagate the chain-catalysed isomerisation of the *N*-hydroxyimino group from **2a** >C=NOH_Z to **2b** >C=NOH_E . Solubility constraints prevented a thorough study of the kinetics above at $[\mathbf{2a}] > 1\text{ mmol dm}^{-3}$ at which the interaction between the iminoxyl radical and the parent oxime would be more obvious. No spectral evidence was obtained for the formation of a possible three-electron bonded radical-adduct in reaction (3), which if formed, must have a very short half-life of <1 μs .



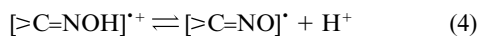
Alternatively, isomerisation of the *N*-hydroxyimino group by the iminoxyl radical may be an outer-sphere process with no adduct involved.

One-electron oxidation of 1-methylindole-3-carboxamide oxime 4a. The absorption spectra of the radicals generated by the oxidation of the amidoxime **4a** by the Br₂^{•-} radical are shown in Fig. 3. At pH 3.5 two absorption maxima are observed

at 335 and 670 nm with extinction coefficients of 2180 and 580 $\text{dm}^3 \text{mol}^{-1} \text{cm}^{-1}$, respectively, which have been attributed to the amidoxime radical cation **4a** [$>\text{C}=\text{NOH}]^{+\bullet}$. Once again at neutral pH the radical cation deprotonates to the neutral iminoxyl radical **4a** [$>\text{C}=\text{NO}]^\bullet$, the spectrum of which is characterised by two absorption maxima at 330 and 580 nm with extinction coefficients of 2170 and 1160 $\text{dm}^3 \text{mol}^{-1} \text{cm}^{-1}$, respectively. As previously observed for the oxime **2a**, the rate of formation of either **4a** [$>\text{C}=\text{NOH}]^{+\bullet}$ or **4a** [$>\text{C}=\text{NO}]^\bullet$ radicals were similar in D_2O and water suggesting that, at pH 7.4, the $\text{Br}_2^{\bullet-}$ radical oxidises the amidoxime by electron transfer to the radical cation which rapidly deprotonates to the iminoxyl radical **4a** [$>\text{C}=\text{NO}]^\bullet$ (see Table 1).

At pH 3.5 and 7.4 and low concentrations of amidoxime **4a**, ca. 0.05–0.1 mmol dm^{-3} , the amidoxime radicals decayed by second-order kinetics, where the rate of decay increased proportionately with the radical concentration, 2–17 Gy. At pH 3.5, the rate constant $2k_{2a} = (1.1 \pm 0.1) \times 10^6 \text{ dm}^3 \text{mol}^{-1} \text{ s}^{-1}$ for the decay of the radical cation **4a** [$>\text{C}=\text{NOH}]^{+\bullet}$ was obtained from the slope of the linear plot of the pseudo-first-order rate constant for the decay of absorption at 720 nm versus initial radical concentration. Acceleration of this rate by a factor of 2.3 to $2k_{2a} = (2.5 \pm 0.1) \times 10^6 \text{ dm}^3 \text{mol}^{-1} \text{ s}^{-1}$ in the presence of 0.5 mol dm^{-3} NaClO_4 was again consistent with our designation of the 720 nm absorption to the radical cation **4a** [$>\text{C}=\text{NOH}]^{+\bullet}$. No salt effect was observed on the rate of decay of the 580 nm absorbing species at pH 7.4 ascribed to the neutral iminoxyl radical. The rate of decay of both **4a** [$>\text{C}=\text{NOH}]^{+\bullet}$ and **4a** [$>\text{C}=\text{NO}]^\bullet$ radicals was independent of $[\text{4a}] \approx 0.05\text{--}2 \text{ mmol dm}^{-3}$.

Acid–base properties of iminoxyl radicals. The different absorption spectra obtained for the oxidation of **2a** and **4a** by the $\text{Br}_2^{\bullet-}$ radical at low and neutral pH (see Figs. 2 and 3) suggest that their corresponding radical cations exist in prototropic equilibrium [reaction (4)] with the iminoxyl radicals.



By measuring the change in absorption at 800 nm as a function of pH 2–9 it was possible to determine the $\text{p}K_a$ of the radical cation **2a** [$>\text{C}=\text{NOH}]^{+\bullet}$. The change of absorption when fitted to the appropriate function gave a $\text{p}K_a = 3.53 \pm 0.03$ for radical cation **2a** [$>\text{C}=\text{NOH}]^{+\bullet}$ (see the insert in Fig. 2). The insert in Fig. 3 shows the increase in absorbance of the iminoxyl radical **4a** [$>\text{C}=\text{NO}]^\bullet$ with increasing pH 2.5–10, which is paralleled by a decline in absorbance of the radical cation **4a** [$>\text{C}=\text{NOH}]^{+\bullet}$ at 750 nm giving a $\text{p}K_a = 5.01 \pm 0.05$. Additional support for the existence of the acid–base equilibrium reaction (4) was obtained by pulse radiolysis of the *O*-methylated analogues of **2a** and **4a**, namely **6** and **5**, respectively. The spectrum for the oxidation of **6** by the $\text{Br}_2^{\bullet-}$ radical is characterised by two absorption maxima at 340 and 720 nm with corresponding extinction coefficients of 3350 and 1450 $\text{dm}^3 \text{mol}^{-1} \text{cm}^{-1}$, respectively. The spectrum was identical over a broad pH range, 2.5–9.4, reflecting the inability of the radical cation **6** [$>\text{C}=\text{NOCH}_3]^{+\bullet}$ to deprotonate. Similarly, the absorption spectra obtained on oxidation of **5** by the $\text{Br}_2^{\bullet-}$ radical was also identical at pH 2.5–9 also indicating that *O*-methylation prevented deprotonation of the radical cation **5** [$>\text{C}=\text{NOCH}_3]^{+\bullet}$ (see Table 1).

Product profiling and quantification

Stable products generated by the one-electron oxidation of 1-methylindole-3-carbaldehyde oxime 2a. Fig. 4 shows typical HPLC traces obtained on the oxidation of the oxime **2a** by the $\text{Br}_2^{\bullet-}$ radical. Table 2 contains the radiation chemical yields for the loss of the parent molecule and the formation of products which were dependent on the concentration of the parent **2a**,

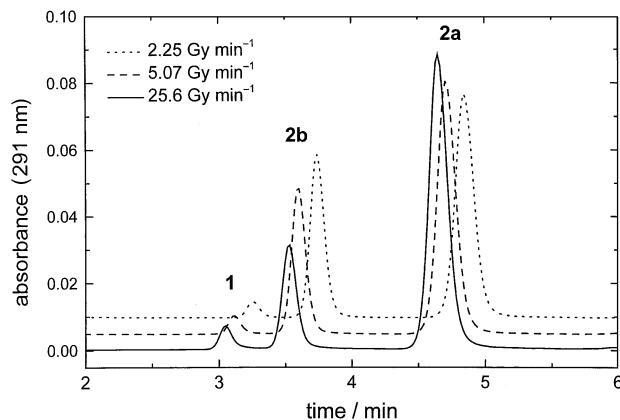


Fig. 4 An HPLC trace obtained from the steady-state γ -radiolysis ($2\text{--}25 \text{ Gy min}^{-1}$) of **2a** ($200 \mu\text{mol dm}^{-3}$) in N_2O -saturated solutions of KBr (50 mmol dm^{-3}) in phosphate buffer (4 mmol dm^{-3}) at pH 7.4.

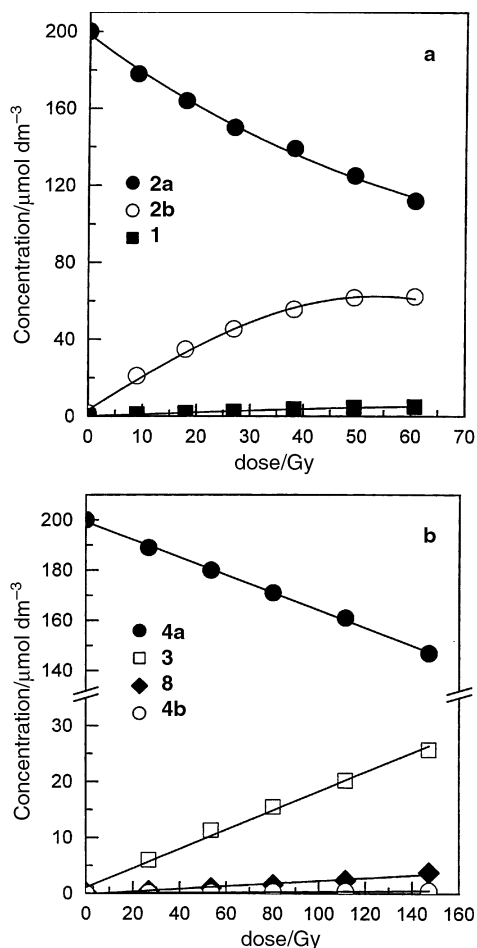
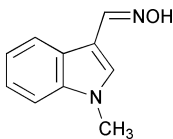


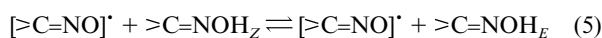
Fig. 5 Oxidation of **2a** (insert a) and **4a** (insert b) by reaction of radiolytically generated $\text{Br}_2^{\bullet-}$ and formation of products at a dose rate of 2.5 Gy min^{-1} at pH 7.4.

rate of radical production and pH. In all experiments performed the oxidation of **2a** generated primarily the isomer denoted **2b** and the aldehyde **1** $>\text{C}=\text{O}$. Fig. 5 shows the non-linear change in concentration of the parent oxime **2a** and products with increasing radiation dose. The corresponding radiation chemical yields G in $\mu\text{mol J}^{-1}$ were estimated from the slope of the initial linear fits to the data between 0 and 10 Gy. Radiation chemical yields for the loss of the parent were usually greater than $G(\text{Br}_2^{\bullet-}) = 0.69 \mu\text{mol J}^{-1}$, which is indicative of a chain reaction. At $200 \mu\text{mol dm}^{-3}$ **2a** and at pH 7.4 lowering the dose rate from 25.5 to 2.3 Gy min^{-1} increased the loss of **2a** from $G(-\text{2a}) = 1.05$ to $1.38 \mu\text{mol J}^{-1}$. Lowering the dose rate also increased the geometric isomerisation of **2a** to **2b** [reaction (5)]

Table 2 Concentration, pH and dose rate effects on the oxidation of the oxime **2a** by the dibromide radical anion^a


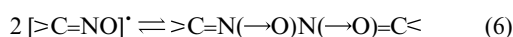
[2a]/mmol dm ⁻³	pH	Dose rate/Gy min ⁻¹	G(- 2a)/μmol J ⁻¹	G(2b)/μmol J ⁻¹	G(1)/μmol J ⁻¹	G(NO ₂ ⁻ /NO ₃ ⁻)/μmol J ⁻¹
0.2	7.41	25.46	1.05 ± 0.05	0.58 ± 0.03	0.124 ± 0.002	—
0.2	7.41	5.1	1.25 ± 0.11	1.23 ± 0.07	0.093 ± 0.003	—
0.2	7.41	2.25	1.38 ± 0.09	1.39 ± 0.15	0.083 ± 0.004	—
0.1	7.38	5.1	0.94 ± 0.09	0.52 ± 0.05	0.121 ± 0.001	0.011 ± 0.002 ^b 0.004 ± 0.003 ^c
0.4	7.38	5.1	1.59 ± 0.24	1.457 ± 0.14	0.077 ± 0.006	—
0.8	7.38	5.1	3.48 ± 0.12	2.780 ± 0.14	0.081 ± 0.001	0.012 ± 0.002 ^b 0.022 ± 0.002 ^c
0.1	3.53	5.1	0.76 ± 0.04	0.62 ± 0.13	0.182 ± 0.001	—
0.1	7.40	5.1	1.16 ± 0.06	0.43 ± 0.01	0.116 ± 0.005	—
0.1	9.46	5.1	1.94 ± 0.31	2.70 ± 0.59	0.061 ± 0.005	—

^a Radiation chemical yield of the dibromide radical anion G(Br₂^{•-}) = 0.69 μmol J⁻¹. ^b NO₂⁻. ^c NO₃⁻.

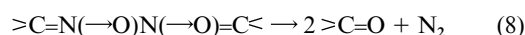
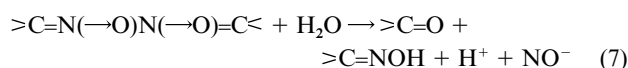


which became stoichiometric at 2.3 Gy min⁻¹. A greater yield of the aldehyde **1** >C=O was obtained at 25.46 Gy min⁻¹ but still only represented ca. 10% of the loss of **2a**. Increasing the concentration of **2a** from 0.1 to 0.8 mmol dm⁻³ increased the loss of parent significantly from G(-**2a**) = 1.25 μmol J⁻¹ to 3.48 μmol J⁻¹ at a dose rate of 5.1 Gy min⁻¹. The results suggest that the Br₂^{•-} radical initiates a chain-propagated turnover of **2a** and greater chain lengths occur by prolonging the lifetime of the **2a** [>C=NO]^{*} radical.

The chemical kinetics have demonstrated that under certain experimental conditions both the radical-cation **2a** [>C=NOH]^{•+} and the iminoxyl radical **2a** [>C=NO]^{*} will decay bimolecularly to products *via* reactions (2a) and (2b), respectively. Although the oxidation of alkyl, dialkyl and aryl oximes can generate stable iminoxyl radical dimers,^{3,7} no such products were detected in the oxidation of **2a**. However, pulse radiolysis of **2a** did show that the decay of **2a** radicals was accompanied by an increase in absorbance between 300 and 400 nm (which was stable up to ca. 30 ms after the electron pulse). More prominent changes in absorbance were observed in the oxidation of the amidoxime **4a** by the Br₂^{•-} radical which is discussed below. In both cases, the observations are consistent with the formation of unstable iminoxyl radical dimers [*e.g.* azine bis-*N*-oxides in reaction (6), although a number of other permutations are pos-



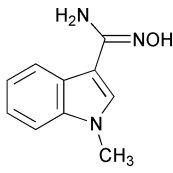
sible depending on the preferred radical coupling position], which are known to absorb at these wavelengths.³ Between pH 3 and 8 the absorbance of the putative dimer species decays in a timescale of seconds to give further products including the aldehyde **1** >C=O. A number of pathways to **1** >C=O from the putative dimer can be envisioned including reactions (7) and (8).



Even utilising experimental conditions which favour aldehyde formation over isomerization, (low concentration of **2a** and high dose rate) the yield of **1** >C=O only accounted for

ca. 12% of the products formed. No evidence was obtained for the generation of the nitroxyl anion (NO⁻) in reaction (7) by standard assays including trapping by thiol to generate the disulfide and hydroxylamine and by the formation of ferrous-nitrosyl complexes with methaemoglobin.³⁰ The low yields (ca. 1%) of nitrite and nitrate measured in the presence of oxygen were below the limits of experimental error. The inability to detect nitrogen oxides in general and the fact that reaction (7) cannot account for the observed balance in radiation chemical yields between the oxidation of **2a** and the products formed suggest that reaction (8) may be the preferred pathway for the formation of the aldehyde **1** >C=O.

Stable products generated by the one-electron oxidation of 1-methylindole-3-carboxamide oxime 4a. Oxidation of the amidoxime **4a** by the Br₂^{•-} radical results in the formation of the nitrile **3**, the amide **8**, the carboxylic acid **7** (generated exclusively at low pH 3.5) plus stable dimers. As with **2a** there was no evidence for nitrogen oxide production from **4a**. The radiation chemical yields for the oxidation of the amidoxime **4a** and formation of these products at different parent concentrations, pH and dose rate are given in Table 3. In marked contrast to the oxidation of the oxime **2a** by the Br₂^{•-} radical, geometric isomerisation of **4a** to **4b** represented only a minor contribution to the loss of the parent under the different experimental conditions employed. At pH 7.4 and a dose rate 5 Gy min⁻¹, an increase in the concentration of **4a** from 0.2 to 1 mmol dm⁻³ resulted in a small increase in the radiation chemical yield for the loss of the amidoxime G(-**4a**) = 0.33 to 0.42 μmol J⁻¹ and an increase in the yield of the isomer G(**4b**) ≈ 0.013 to 0.050 μmol J⁻¹. However, this represents ca. 2% isomerisation of the *N*-hydroxyimino group in **4a** relative to **2a** (see Table 2) under similar experimental conditions. At 0.2 mmol dm⁻³ **4a**, pH 7.4, lowering the dose rate from 25.5 to 2.3 Gy min⁻¹ actually decreased the loss of **4a** from G(-**4a**) = 0.35 to 0.31 μmol J⁻¹. In fact, in the majority of the experiments performed the radiation chemical yields for the loss of the amidoxime **4a** were usually less (ca. 50%) than that expected from G(Br₂^{•-}) = 0.69 μmol J⁻¹ and clearly rules out any significant contribution from a chain reaction. Fig. 5 (lower panel) shows the loss of **4a** and the formation of products which, in marked contrast to **2a** (upper panel), is linear up to ca. 150 Gy. At pH 7.4 and 5 Gy min⁻¹ the loss of the **4a** was not stoichiometric with the quantifiable products, *e.g.* G(-**4a**) = 0.35 μmol J⁻¹ whereas G(**4b** + **3** + **8**) ≈ 0.24 μmol J⁻¹ with ca. 30% products unaccounted for. At lower concentrations of **4a** ([**4a**] = 0.9 mmol dm⁻³) the material balance was better, *e.g.* G(-**4a**) =

Table 3 Concentration, pH and dose rate effects on the oxidation of the amidoxime **4a** by the dibromide radical anion^a


[4a]/mmol dm ⁻³	pH	Dose rate/ Gy min ⁻¹	<i>G</i> (- 4a)/ μmol J ⁻¹	<i>G</i> (4b)/ μmol J ⁻¹	<i>G</i> (3)/ μmol J ⁻¹	<i>G</i> (8)/ μmol J ⁻¹	<i>G</i> (7)/ μmol J ⁻¹	<i>G</i> (NO ₂ ⁻ / NO ₃ ⁻)/μmol J ⁻¹
0.2	7.36	25.46	0.350 ± 0.008	~0.012	0.20 ± 0.004	0.032 ± 0.004	nd	—
0.2	7.36	5.03	0.327 ± 0.010	~0.013	0.17 ± 0.006	0.032 ± 0.004	nd	—
0.2	7.36	2.23	0.313 ± 0.021	~0.014	0.15 ± 0.013	0.024 ± 0.002	nd	—
0.1	7.31	5.03	0.312 ± 0.019	~0.020	0.23 ± 0.021	0.021 ± 0.017	nd	~0.003 ^b ~0.002 ^c
0.5	7.31	5.03	0.384 ± 0.015	~0.041	0.063 ± 0.005	0.049 ± 0.005	nd	—
1.0	7.31	5.03	0.422 ± 0.016	~0.050	0.039 ± 0.004	0.036 ± 0.003	nd	≈0.007 ^b ~0.022 ^c
0.09	3.55	5.02	0.217 ± 0.007	~0.007	0.022 ± 0.001	0.050 ± 0.002	0.092 ± 0.004	—
0.09	7.43	5.02	0.305 ± 0.007	~0.010	0.168 ± 0.006	0.080 ± 0.004	nd	—
0.09	9.49	5.02	0.255 ± 0.005	~0.034	0.243 ± 0.003	0.005 ± 0.001	nd	—

^a Radiation chemical yield of the dibromide radical anion $G(\text{Br}_2^{\cdot-}) = 0.69 \mu\text{mol J}^{-1}$. Not detected = nd. ^b NO₂⁻. ^c NO₃⁻.

0.305 μmol J⁻¹ whereas $G(\mathbf{4b} + \mathbf{3} + \mathbf{8}) \approx 0.26 \mu\text{mol J}^{-1}$ (ca. 15% products unaccounted for).

Pulse radiolysis of **4a** clearly demonstrated that both the radical cation $\mathbf{4a}[\text{>C=NOH}]^{\cdot+}$ and the iminoxyl radical $\mathbf{4a}[\text{>C=NO}]^{\cdot}$ decay bimolecularly to products *via* reactions (2a) and (2b), respectively, and that the associated decay kinetics are independent of [**4a**] up to 1 mmol dm⁻³. It is feasible that these radical–radical reactions generate one or more dimers of varying stability as intermediates to the final products, the nitrile **3**, amide **8** and the carboxylic acid **7**. Some of the peaks formed during γ -radiolysis when analysed by HPLC–MS gave mass ions almost twice that of the parent amidoxime **4a** (e.g. an azine >C=N-N=C< , *m/z* 343) and are therefore likely to be stable iminoxyl radical dimers or products thereof. Unfortunately, it was not possible to synthesize these iminoxyl radical dimers by published synthetic methods (including chemical silver oxide and peroxidase oxidation of **4a**) for full authentication.^{3,8} These putative iminoxyl dimer products absorb more into the visible region of spectrum compared to the amidoxime **4a**. Iminoxyl radicals are capable of dimerising by N–N, N–O, and O–C coupling to generate dimers of varying stability. Possible candidates are the bis-*N*-oxide $\text{C=N(}\rightarrow\text{O)N(}\rightarrow\text{O)=C}$, the azine *N*-oxide $\text{C=N-N(}\rightarrow\text{O)=C}$, $\text{C=N-O-N(}\rightarrow\text{O)=C}$ and C=N-O-C-N=O some of which are known to absorb at around 400 nm.³ However, the $\text{C=N(}\rightarrow\text{O)N(}\rightarrow\text{O)=C}$ group is expected to be very crowded, particularly when bridging two bulky indoles. Consequently, benzaldehyde azine bis-*N*-oxide is unstable in solution and breaks down to benzaldehyde, benzonitrile and benzoic acid, a product profile which is mirrored by the oxidation of the amidoxime **4a** to amide **8**, the nitrile **3** and the carboxylic acid **7**.³

Fig. 3 shows that the decay of both the radical cation and the iminoxyl radical results in an increase in absorbance at ca. 300–600 nm, which is fully formed ca. 16 ms after the electron pulse. It is likely that this absorbance represents the formation of unstable iminoxyl radical dimers. Between 300 and 450 nm this species decays in 250 ms to another product which is stable up to 10 s later. However, at slightly longer wavelengths, ca. 480 nm (where the stable product does not absorb), the rate of decay of this species was found to depend both on the concentration of **4a** and the initial radical concentration. At low doses per pulse (ca. 2 μmol dm⁻³ radicals) the decay is first-order in [**4a**] ≈ 0.1–1 mmol dm⁻³ giving a rate constant for the reaction between iminoxyl radical dimer(s) and **4a** of $k \approx 2 \times 10^3 \text{ dm}^3 \text{ mol}^{-1} \text{ s}^{-1}$. However, at higher doses per pulse (ca. 25 μmol dm⁻³ radicals)

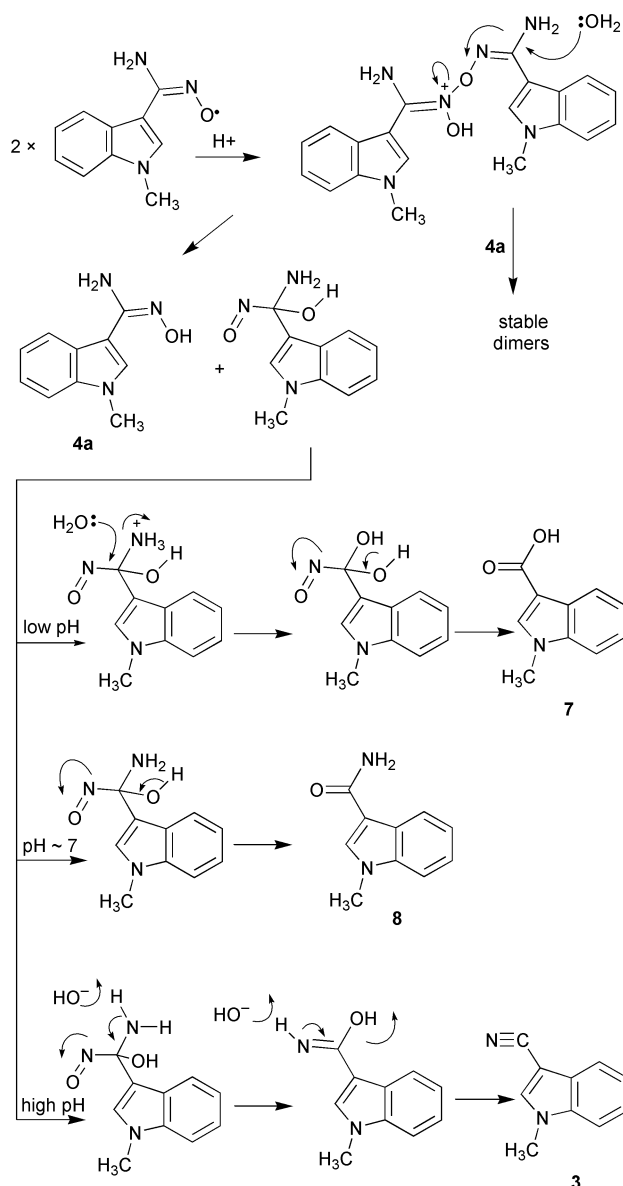
the change in absorbance at 480 nm is independent of the concentration of **4a** up to 1 mmol dm⁻³ where dimer–dimer reactions appear to predominate.

Changing the pH had a significant effect on the products formed in the one-electron oxidation of the amidoxime. When [**4a**] = 0.2 mmol dm⁻³ and the dose rate was 5 Gy min⁻¹ an increase in pH from 7.4 to 9.5 increased the radiation chemical yield of the nitrile $G(\mathbf{3}) = 0.168$ to $0.243 \mu\text{mol J}^{-1}$ and decreased that of the amide $G(\mathbf{8}) = 0.08$ to $0.005 \mu\text{mol J}^{-1}$. The combined yield of these products became stoichiometric with the oxidation of **4a**. However, at low pH = 3.55 an additional product, the carboxylic acid **7**, was formed in higher yield $G(\mathbf{7}) = 0.092 \mu\text{mol J}^{-1}$ than the combined yield of the other quantifiable products $G(\mathbf{3} + \mathbf{4b} + \mathbf{8}) = 0.079 \mu\text{mol J}^{-1}$.

Scheme 2 shows a possible mechanism which may account for observed products at different pHs. The self-reaction of iminoxyl radicals $\mathbf{4a}[\text{>C=NO}]^{\cdot}$ generates a mixture of stable and unstable iminoxyl dimers. The combined radiation chemical yields of the quantifiable products indicate that at low concentrations ([**4a**] ≈ 0.2 mmol dm⁻³) the unstable iminoxyl dimers predominate. Degradation of the dimer (e.g. $\text{C=N-O-N(}\rightarrow\text{O)=C}$) yields the parent **4a** plus a putative intermediate which forms the observed products: the carboxylic acid **7** at low pH, the amide **8** at neutral pH, and the nitrile **3** at higher pH. Although the NO⁻ anion is likely to be a by-product of these reactions, the assays employed for its direct measurement have to out-compete the rapid decay of two NO⁻ anions to N₂O. Schemes can be drawn for the decay of azine bis-*N*-oxides to the observed products at different pHs without the formation of NO⁻ although these pathways cannot account for the regeneration of the parent amidoxime **4a**. The reason why iminoxyl radicals should generate a mixture of stable and unstable dimers is unclear. However, when [**4a**] = 1 mmol dm⁻³ the combined radiation chemical yield $G(\mathbf{3} + \mathbf{4b} + \mathbf{8}) = 0.13 \mu\text{mol J}^{-1}$ is far less than $G(-\mathbf{4a}) = 0.42 \mu\text{mol J}^{-1}$ suggesting that the unstable dimers formed initially can react with **4a** to form the more stable dimers detectable by HPLC.

Conclusions

One-electron oxidation of the oxime **2a** and the amidoxime **4a** by the dibromide radical anion in aqueous solution yields radical cations which deprotonate to give iminoxyl-type radicals at neutral pH. The ratios of the rates of reaction of the dibromide radical anion with the oximes in H₂O and D₂O solutions are



Scheme 2 Possible mechanism for the formation of products from the one-electron oxidation of the amidoxime **4a**.

close to unity both above and below the pK_a of the radical cations. Since hydrogen atom abstraction from the *N*-hydroxyimino moiety would be expected to differ by a factor of *ca.* 2 in the two solvents it is concluded that oxidation occurs by electron transfer. Unequivocal demonstration that the observed spectral changes were due to deprotonation from the *N*-hydroxyimino moiety was made from comparative experiments with indole oximes **2a** and **4a** (in which possible deprotonation to indolyl radicals is prevented by *N*¹-methylation) and their corresponding *O*-methylated derivatives. With the *O*-methylated compounds **5** and **6** the spectra were found to be pH-dependent over a wide range implying that deprotonation of the radical cations takes place from the *N*-hydroxyimino moiety. An increase in the radical cation pK_a by *ca.* 1.5 pH units occurs when the α -hydrogen atom in **2a** is substituted by an amino group to give **4a**. The exact electron distribution within the radicals is uncertain and the radical cations and iminoxyl radicals have therefore been referred to throughout as $[>C=NOH]^+$ and $[>C=NO]^\cdot$, respectively.

α -Amino substitution significantly modifies the product profile in the oxidation of **4a** from that of **2a**. The iminoxyl radicals decayed bimolecularly *via* unstable dimers to the aldehyde especially at low concentrations of **2a** and high dose rates, with higher concentrations of **2a** and lower dose rates favouring the

chain-catalysed isomerisation of the *N*-hydroxyimino moiety. Radicals from **4a** decay bimolecularly to form unstable dimers which degrade to produce an amide, nitrile, and carboxylic acid depending on the pH.

This work highlights the exploitation of radiation chemistry and radiation chemical techniques in the characterisation of the physico-chemical properties of iminoxyl radicals.

Experimental

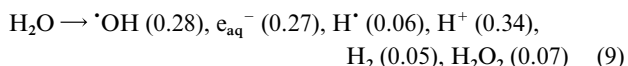
Materials

Potassium bromide, sodium or potassium phosphate salts, and potassium thiocyanate were from Merck and were of analytical quality. Deuterium oxide (heavy water, 99.9% D) was obtained from Sigma–Aldrich (Dorset, UK). Solutions were prepared with water purified by a Milli-Q system (Millipore). Before irradiation, solutions were bubbled with zero-grade nitrous oxide (N_2O , oxygen content <10 ppm) or with N_2O-O_2 (80 : 20%) mixtures (British Oxygen Company). 1-Methylindole-3-carbaldehyde oxime derivatives and putative oxidation products were prepared by derivation of commercially available indoles (Sigma–Aldrich, Dorset, UK). All experiments were performed at room temperature ($20 \pm 2^\circ C$).

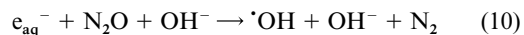
Radiation chemistry

The pulse radiolysis experiments were performed with a 6 MeV linear accelerator as described previously.²¹ A pulse of 0.5 μs delivered doses of 1–35 Gy, as determined by thiocyanate dosimetry.³¹ Steady-state irradiations were performed with a ⁶⁰Co γ -source with a nominal activity of 2000 Ci. The solutions were irradiated in air-tight vials at dose rates in the range 2–25 Gy min^{-1} , as determined by Fricke dosimetry.³² Radiation chemical yields (*G*) in $\mu mol J^{-1}$ for the loss of the parent molecule and formation of products were calculated from the slope of plots of change in concentration *versus* radiation dose.

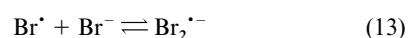
The dibromide radical anion ($Br_2^{\cdot-}$) was generated by radiolysis of N_2O -saturated solutions of KBr (50 $mmol dm^{-3}$) in phosphate buffer (4 $mmol dm^{-3}$). Under these conditions, the radiolysis of water generates radical, ions, and molecular products [reaction (9)]. (The numbers in parentheses are the



radiation chemical yields in $\mu mol J^{-1}$.) The hydrated electron (e_{aq}^-) reacts with N_2O and is converted into the hydroxyl radical ($\cdot OH$), which becomes the main primary product of water radiolysis [reaction (10)]. The $Br_2^{\cdot-}$ radical anion is then



rapidly formed (<0.5 μs) by the sequence of reactions [reactions (11)–(13)].^{27,33}



In pulse radiolysis experiments the reaction of the $Br_2^{\cdot-}$ radical anion with the oxime derivatives was monitored by absorption spectroscopy and the extinction coefficients of the transient species were calculated using the value 0.69 $\mu mol J^{-1}$ for the radiation chemical yield of the $Br_2^{\cdot-}$ radical anion.³⁴

Synthetic chemistry

NMR spectra were obtained at 60 MHz with a JEOL MY60 spectrometer and SiMe₄ as internal standard. Elemental analyses were determined by MEDAC Ltd., Brunel Science Centre, Egham, Surrey, UK TW20 0JZ, and all compounds were chromatographically homogeneous by TLC and HPLC–MS (Waters, Watford, UK). Solutions in organic solvents were dried by standard procedures and dimethylformamide (DMF) and tetrahydrofuran (THF) were anhydrous commercial grades. Silica gel for flash column chromatography was Merck Kieselgel 60 H grade (230–400 mesh). Melting points were determined on a Thomas Hoover melting point apparatus and are uncorrected.

1-Methylindole-3-carbaldehyde oxime 2a

Indole (3.0 g, 0.026 mol) was dissolved in DMF (30 cm³) and sodium hydride (0.88 g of a 60% dispersion, 22 mmol) was gradually added with stirring under a nitrogen atmosphere. After 1 h at ambient temperature methyl iodide (30 cm³, 92.6 mmol) was added and the solution stirred for 2 h, then poured onto a solution of sodium hydrogen sulfate (10%, 500 cm³). The product was extracted with ethyl acetate and washed with water (3 × 250 cm³) and saturated sodium bicarbonate solution (250 cm³), dried and evaporated. The residue was added to a previously prepared solution of DMF (11.4 g, 15.5 mmol) which had been cooled to 0 °C, phosphorus oxychloride (5.2 g, 33.4 mmol) was added dropwise, and the mixture was stirred for 0.5 h. The reaction mixture was then stirred for 18 h at ambient temperature, poured onto ice (250 g) and sodium hydroxide (37%, 100 cm³) added. The product was extracted with ethyl acetate and purified on silica, eluting with ethyl acetate–hexane, 1 : 1, to give 1-methylindole-3-carbaldehyde (1.0 g, 24%) as a white solid, mp 68–70 °C. ¹H NMR (CDCl₃) δ 9.94 (1 H, s), 8.3 (1 H, m), 7.58 (1 H, s), 7.32 (3 H, m), 3.81 (3 H, s).

Hydroxylamine hydrochloride (10.2 g, 147 mmol) was dissolved in ethanol (125 cm³) and sodium hydroxide (5.0 g, 125 mmol in 125 cm³ ethanol) was added with stirring. After 1.5 h the solution was filtered and the filtrate added to a solution of 1-methylindole-3-carbaldehyde (10.0 g, 62.9 mmol) in ethanol (250 cm³). The solution was heated at 60 °C for 24 h, cooled and evaporated. The residue was purified on silica gel (eluting with dichloromethane and then ethyl acetate) to give 7.1 g (65%) of 1-methylindole-3-carbaldehyde oxime **2a** as a white solid, mp 144–146 °C (lit.,³⁵ 138–140 °C). ¹H NMR (CDCl₃) δ 8.17 (1 H, s), 7.67 (2 H, m), 7.22 (3 H, m), 3.75 (3 H, s). MS (EI) *m/z* (relative intensity) 174 (M⁺, 100%), 156 (44), 142 (47), 131 (97), 115 (14), 103 (11) (Calc. for C₁₀H₁₀N₂O: C, 68.9; H, 5.8; N, 16.1. Found: C, 68.8; H, 5.8; N, 16.1%).

1-Methylindole-3-carboxamide oxime 4a

1-Methylindole-3-carbaldehyde oxime **2a** (10.0 g, 57.5 mmol) was dissolved in acetic anhydride (100 cm³) together with sodium acetate (10 g, 122 mmol). The solution was then heated at 100 °C for 4 h, cooled and evaporated. The residue was purified on silica, eluting with ethyl acetate–hexane (1 : 3) to give 3-cyano-1-methylindole **3** (5.2 g, 58%) as a yellow oil, ¹H NMR (CDCl₃) δ 7.09–7.43 (5 H, m), 3.60 (3 H, s). Hydroxylamine hydrochloride (1.51 g, 21.7 mmol) was dissolved in methanol (100 cm³) and potassium hydroxide (1.21 g, 21.7 mmol) was added with stirring. After 1.5 h the solution was filtered and the filtrate added to a solution of **3** (0.6 g, 3.9 mmol) in ethanol (30 cm³). The solution was heated at 100 °C for 18 h, cooled and evaporated. The residue was purified on silica (eluting with ethyl acetate) to give 0.26 g (35%) of 1-methylindole-3-carboxamide oxime **4a** as a white solid, mp 149–150 °C (lit.,³⁶ 189–190 °C). ¹H NMR [(CD₃)₂SO] δ 9.16 (1 H, s), 8.05 (1 H, d), 7.43 (2 H, s), 6.94–7.16 (3 H, m), 5.51 (1 H, br s), 3.75 (3 H, s). MS (EI) *m/z* (relative intensity) 189 (M⁺, 100%), 172 (72), 157

(60), 142 (20), 131 (33), 103 (12) (Calc. for C₁₀H₁₁N₃O₃·H₂O: C, 59.7; H, 6.1; N, 20.9. Found: C, 59.7; H, 5.6; N, 20.9%).

O,1-Dimethylindole-3-carboxamide oxime 5

Carboxamide oxime **4a** (0.2 g, 1.1 mmol) and trimethyl-oxonium tetrafluoroborate (1.0 g, 6.76 mmol) were dissolved in dichloromethane (10 cm³) and tetrahydrofuran (2 cm³) and the solution stirred for 24 h at ambient temperature. Ethyl acetate (50 cm³) was then added and the solution washed with saturated sodium bicarbonate solution (50 mM) and brine, dried and evaporated. The residue was purified by flash column chromatography eluting with ethyl acetate followed by radial chromatography (4 mm plate eluting with hexane–ethyl acetate, 2 : 1) to give **5** (13 mg, 5.8%) as a pale yellow oil. LC–MS, 96.4%, MS (EI) *m/z* (relative intensity) 203 (M⁺, 100%), 172 (37), 157 (40), 131 (37).

O,1-Dimethylindole-3-carbaldehyde oxime 6

Compound **2a** (174 mg, 1 mmol) was dissolved in DMF (5 cm³) and sodium hydride (50 mg of a 60% dispersion, 1.2 mmol) was added with stirring and under nitrogen. The solution was heated at 50 °C for 0.5 h, cooled and methyl iodide (1 cm³, 16.1 mmol) added. The solution was then heated at 60 °C for 0.5 h, cooled and sodium hydrogen sulfate (10%, 15 cm³) added. The solution was extracted with ethyl acetate, washed with sodium bicarbonate and brine, dried and evaporated. The residue was purified on silica gel, eluting with ethyl acetate–hexane 2 : 1, to give **6** (50 mg, 27%) as a pale yellow oil. ¹H NMR (CDCl₃) δ 8.03 (1 H, s), 7.83 (1 H, m), 7.29 (4 H, m), 4.08 (3 H, s), 3.80 (3 H, s). MS (EI) *m/z* (relative intensity) 188 (M⁺, 100%), 157 (43), 142 (54), 130 (28), 115 (14), 103 (14).

1-Methylindole-3-carboxamide 8

Methyl indole-3-carboxylate (3.0 g, 17.15 mmol) was dissolved in THF (50 cm³) and sodium hydride (1.1 g of a 60% dispersion, 24.4 mmol) added with stirring under nitrogen. Methyl iodide (10 cm³, 161 mmol) was then added and the solution heated at 60 °C for 1 h, cooled and poured onto sodium hydrogen sulfate (10%, 100 cm³). The solution was extracted with ethyl acetate and washed with sodium bicarbonate and brine, dried and evaporated. The residue was triturated with ether and the solid collected and washed with ether, to give 2.6 g (80%) of methyl 1-methylindole-3-carboxylate, mp 88–90 °C. ¹H NMR (CDCl₃) δ 8.13 (1 H, m), 7.68 (1 H, s), 7.26 (3 H, s), 3.87 (3 H, s), 3.77 (3 H, s). MS (EI) *m/z* (relative intensity) 189 (M⁺, 70%), 158 (100), 148 (5), 130 (18), 115 (2), 103 (7). This material (2.6 g, 13.8 mmol) was dissolved in a solution of potassium hydroxide (1 M, 100 cm³) in acetonitrile (100 cm³) and the solution heated under reflux for 1.5 h. The solution was cooled and acidified with 1 M HCl and the resulting white precipitate collected and washed with water, to give 1-methylindole-3-carboxylic acid (2.4 g, 100%), mp 202–203 °C. ¹H NMR (CDCl₃) δ 8.18 (1 H, m), 8.04 (1 H, s), 7.47 (3 H, m), 3.89 (3 H, s). MS (EI) *m/z* (relative intensity) 175 (M⁺, 100%), 158 (70), 130 (16), 103 (7).

1-Methylindole-3-carboxylic acid (1.0 g, 5.7 mmol) was dissolved in DMF (50 cm³) together with *N,N'*-carbonyldiimidazole (0.92 g, 5.7 mmol). The solution was stirred for 12 h at 20 °C and then ammonia gas bubbled through the solution for 2.5 h. Water (50 cm³) was added and the solution extracted with ethyl acetate and washed with brine, dried and evaporated. The residue was purified on silica eluting with ethyl acetate to give 0.84 g (85%) of 1-methylindole-3-carboxamide **8** as a white solid, mp 176–177 °C (lit.,³⁷ 176 °C). ¹H NMR (CDCl₃) δ 8.32 (1 H, m), 7.95 (1 H, s), 7.17 (3 H, m), 3.85 (3 H, s), 3.0 (2 H, s). MS (EI) *m/z* (relative intensity) 174 (M⁺, 68%), 158 (100), 130 (12), 103 (12) (Calc. for C₁₀H₁₀N₂O: C, 68.9; H, 5.8; N, 16.1. Found: C, 68.5; H, 5.8; N, 16.0%).

HPLC detection of products

Product analysis following γ -radiolysis of **2a** and **4a** was performed by separation on a 100 mm \times 3.2 mm base-deactivated reversed-phase column (Hichrom RPB, Hichrom, Reading, UK) at a flow rate of 1 cm³ min⁻¹. The products from the oxidation of the oxime **2a** were eluted isocratically with 35% methanol, 7.5% acetonitrile, 57.5% water. The products of the amidoxime **4a** were eluted with mixtures of (A) heptanesulfonic acid (5 mmol dm⁻³), KH₂PO₄ (5 mmol dm⁻³), H₃PO₄ (5 mmol dm⁻³) and (B) 75% acetonitrile, 25% water with a linear gradient of 25–65% B, in 5 min. Eluted peaks were detected by absorption at 265 and 292 nm using a Waters 996 diode array detector (Watford, UK) and concentrations were determined from peak areas using Waters Millennium Software.

Ground state pK_as were determined by chromatographing either **2a** or **4a** in citrate buffers of different pH, and measuring the retention time. Protonation of the hydroxyamino group in **2a** and **4a** occurred at low pH with pK_a(RR₁C=NOH + H⁺ \rightleftharpoons RR₁C=NHOH⁺) = 2.3 \pm 0.1 and 3.5 \pm 0.1, respectively. No further changes in retention time for either **2a** or **4a** were observed between pH 4 and 9 implying that pK_a(RR₁C=NOH \rightleftharpoons RR₁C=NO⁻ + H⁺) > 9.

Nitrite and nitrate were determined by reversed-phase HPLC with ion-pairing using tetrabutylammonium hydroxide, with UV detection at 214 nm as described previously.³⁸

Acknowledgements

The authors wish to thank Drs Peter Thomson and Sharon Rossiter for helpful discussions. This work is supported by the Cancer Research Campaign [CRC] and the Gray Cancer Institute [GCI].

References

- 1 J. R. Thomas, *J. Am. Chem. Soc.*, 1964, **86**, 1446.
- 2 J. L. Brokenshire, G. D. Mendenhall and K. U. Ingold, *J. Am. Chem. Soc.*, 1971, **93**, 5278.
- 3 J. L. Brokenshire, J. R. Roberts and K. U. Ingold, *J. Am. Chem. Soc.*, 1972, **94**, 7040.
- 4 G. D. Mendenhall and K. U. Ingold, *J. Am. Chem. Soc.*, 1973, **95**, 2963.
- 5 A. Alberti, G. Barbaro, A. Battaglia, M. Guerra, F. Bernardi, A. Dondoni and G. F. Pedulli, *J. Org. Chem.*, 1981, **46**, 742.
- 6 A. R. Jaszewski, J. Jezierska, M. Krowicka and E. Kalecinska, *App. Magn. Reson.*, 2000, **18**, 85.
- 7 C. Lagercrantz, *Acta Chem. Scand.*, 1988, 414.
- 8 K. Fukunishi, K. Kidata and I. Naito, *Synthesis*, 1991, 237.

- 9 B. C. Gilbert and R. O. C. Norman, *J. Chem. Soc. B*, 1966, 86.
- 10 Y. Sanakis, C. Goussias, R. P. Mason and V. Petrouleas, *Biochemistry*, 1997, **36**, 1411.
- 11 M. R. Gunther, L. C. Hsi, J. F. Curtis, J. K. Gierse, L. J. Marnett, T. E. Eling and R. P. Mason, *J. Biol. Chem.*, 1997, **272**, 17086.
- 12 H. G. Korth, R. Sustmann, C. Thater, A. R. Butler and K. U. Ingold, *J. Biol. Chem.*, 1994, **269**, 17776.
- 13 D. J. Tantillo, J. M. Fukuto, B. M. Hoffman, R. B. Silverman and K. N. Houk, *J. Am. Chem. Soc.*, 2000, **122**, 536.
- 14 A. Jousserandot, J.-L. Boucher, Y. Henry, B. Niklaus, B. Clement and D. Mansuy, *Biochemistry*, 1998, **37**, 17179.
- 15 B. Clement, J.-L. Boucher, D. Mansuy and A. Harsdorf, *Biochem. Pharmacol.*, 1999, **58**, 439.
- 16 A. Renedon-Cornière, J.-L. Boucher, S. Dijols, D. J. Stuehr and D. Mansuy, *Biochemistry*, 1999, **38**, 4663.
- 17 M. L. Posener, G. E. Adams, P. Wardman and R. B. Cundall, *J. Chem. Soc., Faraday Trans. 1*, 1976, **72**, 2231.
- 18 X. Shen, J. Lind and G. Merényi, *J. Phys. Chem.*, 1987, **91**, 4403.
- 19 S. V. Jovanovic, S. Steenken and M. G. Simic, *J. Am. Chem. Soc.*, 1991, **95**, 684.
- 20 S. V. Jovanovic and S. Steenken, *J. Phys. Chem.*, 1992, **96**, 6674.
- 21 L. P. Candeias, L. K. Folkes, M. F. Dennis, K. B. Patel, S. A. Everett, M. R. L. Stratford and P. Wardman, *J. Phys. Chem.*, 1994, **98**, 10131.
- 22 L. P. Candeias, in *The Chemistry of N-Centered Radicals*, ed. Z. Alfassi, Wiley, New York, 1998, p. 577.
- 23 R. Santus and L. I. Grossweiner, *Photochem. Photobiol.*, 1972, **15**, 101.
- 24 S. Solar, N. Getoff, P. S. Surdhar, D. A. Armstrong and A. Singh, *J. Phys. Chem.*, 1991, **95**, 3639.
- 25 J. W. Janes, B. S. Potter, M. A. Naylor, A. C. Ferguson, K. B. Patel, M. R. L. Stratford, P. Wardman and S. A. Everett, *Acta Crystallogr., Sect. C*, 2001, **57**, 312.
- 26 D. N. Nicolaides and E. A. Varella, in *The Chemistry of Acid Derivatives: Supplement B*, ed. S. Patai, Wiley, Oxford, 1992, Vol. 2, p. 875.
- 27 D. Zehavi and J. Rabani, *J. Phys. Chem.*, 1972, **76**, 312.
- 28 *CRC Handbook of Chemistry and Physics*, ed. D. R. Lide, 73rd edn., CRC Press, London, 1986.
- 29 B. Perlmutter-Hayman, *Prog. React. Kinet.*, 1971, **6**, 239.
- 30 M. P. Doyle, S. N. Mahapatro, R. D. Broene and J. K. Guy, *J. Am. Chem. Soc.*, 1988, **110**, 593.
- 31 G. V. Buxton and C. R. Stuart, *J. Chem. Soc., Faraday Trans.*, 1995, **91**, 279.
- 32 K. Sehested, O. L. Rasmussen and H. Fricke, *J. Phys. Chem.*, 1968, **72**, 626.
- 33 A. Mamou, J. Rabani and D. Behar, *J. Phys. Chem.*, 1977, **81**, 1447.
- 34 R. H. Schuler, A. L. Hartzell and B. Behar, *J. Phys. Chem.*, 1981, **85**, 192.
- 35 S. Hirmath, S. Thaker and M. Purohit, *Indian J. Chem. B*, 1984, **23**, 926.
- 36 C. Swain, R. Baker, C. Kneen, J. Moseley, J. Saunders, E. M. Seward, M. St. Beer, J. Stanton and K. Watling, *J. Med. Chem.*, 1991, **34**, 140.
- 37 U. Pindur and M. Kim, *Tetrahedron*, 1989, **45**, 6427.
- 38 M. R. L. Stratford, *Methods Enzymol.*, 1999, **301**, 259.